ORGANOMETALLICS

ARTICLE

pubs.acs.org/Organometallics

Remote Substitution on *N*-Heterocyclic Carbenes Heightens the Catalytic Reactivity of Their Palladium Complexes

Benjamin R. Dible, Ryan E. Cowley, and Patrick L. Holland*

Department of Chemistry, University of Rochester, Rochester, New York 14627, United States

Supporting Information

ABSTRACT: A new series of exceptionally bulky *N*-heterocyclic carbene (NHC) ligands is based on 1,3-bis-2′,6′-diisopropylphenylimidazol-2-ylidene (IPr), through substitution of large groups at the para (4′) position of the aryl rings. π-Cinnamylpalladium chloride complexes with these ligands are pre-catalysts for Suzuki−Miyaura coupling. Large triarylmethyl substituents at the 4′ position of the NHC give significantly greater catalyst activity. Although the $\%V_{bur}$ parameter has been proposed as a general measure of the size of bulky ligands, the sterically induced enhancement of the catalytic rate does not correlate with the $\%V_{bur}$ parameter; instead, solid angles are more useful in quantifying the differences between ligands because they account for bulk more distant from the metal. Overall, these results show that the use of distant steric hindrance can have a distinct positive influence on catalytic ability.

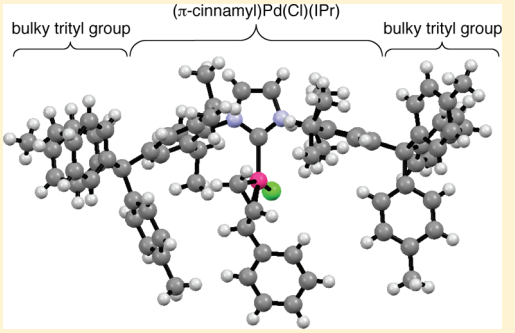

INTRODUCTION

The *N*-heterocyclic carbene (NHC) ligands have been used widely in catalysis and in coordination chemistry, where they serve as extremely strong σ-donors that modify the steric and electronic environment of the metal center. The study of NHC complexes has become a rich area that has attracted considerable interest, as evidenced by the large number of publications and reviews relating to NHC complexes.[1−5]

To better describe and predict the properties of NHC complexes, chemists have developed several methods to quantify characteristics in terms of both sterics and electronics.[6] Work by Nolan[7] and by Crabtree[8] used the Tolman electronic parameter (TEP) to describe the σ-donating abilities of NHC ligands. The TEP method compares the CO stretching frequencies of tetrahedral $(NHC)Ni(CO)_3$ complexes to those for $(R_3P)Ni(CO)_3$ complexes.[9] However, this method of determining TEP values was limited, because large NHC ligands, such as I*t*Bu and IAd, give planar $(NHC)Ni(CO)_2$ complexes that are not directly comparable to the reference tetrahedral tricarbonylnickel complexes. To avoid this problem, Crabtree and co-workers developed a method for calculating TEP values based on the carbonyl stretching frequencies for iridium complexes.[8] This development is advantageous because it facilitates TEP determination in a wider range of NHCs and because it circumvents the use of hazardous $Ni(CO)_4$.

Although TEP values are generally accepted as the best method for quantifying electronic effects of ligands, the description of ligand steric effects has been more controversial. The Tolman cone angle[9] is a starting point for describing ligand sterics. The Tolman cone angle is obtained by treating the ligand as a cone with the metal center acting as the vertex and measuring the resulting angle, or weighted average of angles for nonsymmetrical ligands. In the discussion of NHC steric effects, the most commonly discussed steric parameter is the percent buried volume ($\%V_{bur}$), which defines a sphere around the inner part of a complex, and measures the fraction of the *volume* of this sphere occupied by the ligand.[10] The use of $\%V_{bur}$ in quantifying the size of NHC ligands has been established by a body of work by Cavallo and Nolan.[11]

We were interested in developing NHC ligands with the intent of not only shielding the close environment of a metal center but also projecting far from the metal center to prevent dimerization and/or aggregation of complexes. To accomplish this goal in the case of the useful NHC ligands, we designed a series of new ligands with large remote substituents, which are described in this paper. We show below that the size of these ligands is not predicted by the $\%V_{bur}$ parameter, and use another steric measure that better quantifies the steric variation. To demonstrate the impact of the remote substituents on catalyst activity with a well-known catalyst system, we also describe the influence of the remote substitution on the rate and conversion of catalytic Suzuki−Miyaura coupling by $(NHC)(\pi\text{-cinnamyl})PdCl$ complexes incorporating the new ligands.[12]

RESULTS AND DISCUSSION

Ligand Synthesis and Palladium Complex Formation. To evaluate the effects of remote, sterically demanding groups on ligand properties, we chose IPr as the parent ligand upon which to build. The synthesis begins with triarylmethanols **1b**−**1d** as protoelectrophiles to derivatize 2,6-diisopropylaniline **2a** at the 4-position via electrophilic aromatic substitution. This approach

Received: April 24, 2011
Published: September 08, 2011

is advantageous because the triarylmethanols are simple to prepare. Furthermore, the use of triarylmethanols as electrophile precursors for electrophilic aromatic substitution reactions with anilines is well-precedented.[13,14] Thus, treatment of known triarylmethanols **1b**−**1d** with an excess of aniline **2a** in the presence of HCl produces trityl anilines **2b**−**2d** cleanly and in high yield (Scheme 1), as long as the reaction is performed under an inert atmosphere. A basic workup is required to avoid product contamination with anilinium salts.

With trityl anilines **2b**−**2d** and 4-(1′-adamantyl)aniline **2e** in hand, the remainder of the ligand synthesis may be addressed. The procedures developed by Nolan for the synthesis of IPr·HCl[15] and by Herrmann for the synthesis of IPr·HBF_4[16] required several modifications to produce the new ligands, due to solubility and stability differences. The first step in the synthesis of IPr is the condensation of aniline **2a** with glyoxal in ethanol at room temperature, which produces α-diimine **3a** as a yellow precipitate. Diimine **3a** is then isolated by filtration and washed with methanol, presumably in order to remove unreacted **2a**. However, unlike **2a**, anilines **2b**−**2e** are not very soluble in ethanol at room temperature, so it is necessary to perform the condensation reactions at lower concentrations and at an elevated temperature of 80 °C. Under these modified conditions, α-diimines **3b**−**3e** form readily. Purification of α-diimines **3b**−**3e** is problematic, so the crude products are carried on to the next step as long as the ratio of product **3** to aniline **2** is ≥9:1. In cases where the ratio is lower than 9:1, the mixture is subjected to the condensation conditions a second time in order to enrich the material. Partial characterization for α-diimines **3b**−**3e** is given here for convenience, but it must be noted that these compounds are typically obtained in only 90−95% purity.

Condensation of α-diimines **3b**−**3e** with paraformaldehyde and $HBF_4 \cdot Et_2O$ provides imidazolium tetrafluoroborates **4b**−**4e**, in direct analogy to the literature preparation of IPr·HBF_4 salt **4a**.[16] However, the workup is modified significantly for the para-substituted anilines. IPr·HBF_4 salt **4a** is typically purified via filtration, followed by washing the crude solid with THF.[16] Unlike IPr·HBF_4 salt **4a**, imidazolium salts **4b**−**4d** are soluble in THF. Furthermore, the major contaminant in crude salts **4b**−**4d** appears to be the HBF_4 salts of the parent diimines **3b**−**3d**. Diimines **3a**−**3e** undergo a color change from yellow to red upon the addition of $HBF_4 \cdot Et_2O$ in toluene. In the reaction of diimine **3a** to produce IPr·HBF_4, the reaction mixture eventually turns brown and attempts to recover unreacted **3a** were not successful. However, in the reactions of **3b**−**3e** under analogous conditions, the red color persists until the reaction mixture is treated with aqueous bicarbonate, at which point the yellow color characteristic of α-diimines **3a**−**3e** returns. Furthermore, an attempt to prepare NHC salt **4d** proceeded with less than 15% yield, and 58% of α-diimine **3d** is recovered. Though attempts to fully characterize this red protonated intermediate have not been successful, a broad peak at δ 8.2 ppm and a significantly downfield shifted septet at δ 3.2 ppm are observed in the crude spectrum of NHC salt **4d** prior to basic workup, consistent with the presence of a protonated intermediate.

These observations suggest that the decomposition of **3** under acidic conditions might be the yield-limiting factor in the synthesis of IPr salts. If so, then the yields of NHC salts **4b**−**4e** should be significantly higher than for **4a**. However, the yields are similar to those reported for IPr·HCl and IPr·HBF_4 (Scheme 2). Another potential explanation for the low yields of NHC salts is that diimine protonation inhibits cyclization. In a test of this hypothesis, the formation of **4d** using an excess of paraformaldehyde and only one equivalent of acid, results in an improved yield of 61%. However, applying these conditions to the synthesis of IPr **4a** gives an unimproved yield of 35%, suggesting that the yield-limiting factors for IPr **4a** are not the same as those for the other NHCs. Finally, adding 0.25 equiv of iPr_2NEt as a potential buffer has deleterious results on the yield. Either iPr_2NEt does not have the correct pK_a to buffer this

Scheme 1. Preparation of Trityl-Substituted Anilines

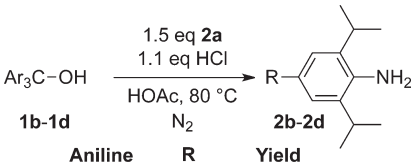

Aniline	R	Yield
2b	Ph_3C	76%
2c	$(4\text{-MePh})_3C$	93%
2d	$(4\text{-}t\text{BuPh})_3C$	97%

Scheme 2. Preparation of NHC·HBF_4 Salts via Sequential Condensations

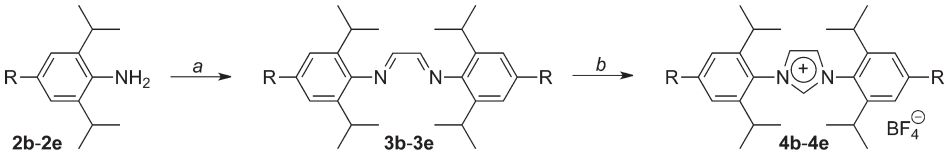

R	Product	Yield	Product	Yield
H	**3a**		**4a**[c]	35%
Ph_3C	**3b**	89%	**4b**	35%
$(4\text{-MePh})_3C$	**3c**	99%	**4c**	28%
$(4\text{-}t\text{BuPh})_3C$	**3d**	90%	**4d**	35%
			4d[c]	61%
			4d[d]	18%
1-adamantyl	**3e**	74%	**4e**	20%

a) HCO_2H (cat), 0.5 eq glyoxal, EtOH, 80 °C
b) 1.0 eq $(CH_2O)_n$, 1.5 eq $HBF_4 \cdot Et_2O$, PhMe
c) 1.25 eq $(CH_2O)_n$, 1.0 eq $HBF_4 \cdot Et_2O$, PhMe
d) 1.1 eq $(CH_2O)_n$, 1 eq $HBF_4 \cdot Et_2O$, 0.25 eq iPr_2NEt, PhMe

dx.doi.org/10.1021/om200349y |*Organometallics* 2011, 30, 5123–5132

Scheme 3. Preparation of NHC-π-CinnamylPdCl Complexes

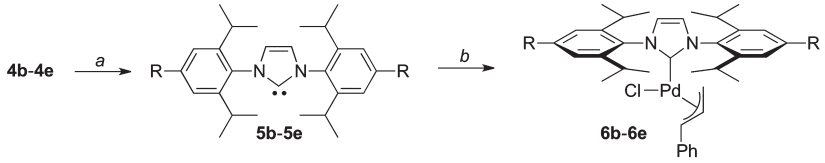

R	Product	Yield	Product	Yield
H	**5a**		**6a**	
Ph_3C	**5b**	93%	**6b**	98%
$(4\text{-MePh})_3C$	**5c**	>99%	**6c**	66%
$(4\text{-}t\text{BuPh})_3C$	**5d**	>99%	**6d**	82%
1-adamantyl	**5e**	78%	**6e**	94%

a) 1.1 eq KO*t*Bu, PhMe b) 0.5 eq $[\text{cinPdCl}]_2$, PhMe

reaction or the problem is more complicated than diimine protonation-inhibited cyclization.

Imidazolium salts **4b**−**4e** may be deprotonated with potassium *tert*-butoxide under N_2 to generate NHCs **5b**−**5e**. Although it is common to generate and use NHCs in situ when preparing π-allylpalladium complexes, isolating the NHCs prior to ligation allows for a final purity check prior to the use of precious metals. Here, each free NHC has been characterized using NMR spectroscopy and elemental analysis.

The final step in the synthesis is to break up the chloro-bridged dimer $[(\pi\text{-cinnamyl})\text{PdCl}]_2$ by treatment with the NHC. In the process of performing these reactions, we obtained an X-ray quality crystal of $[(\pi\text{-cinnamyl})\text{PdCl}]_2$, which is presented in the Supporting Information. Treatment of the palladium dimer with each NHC **5b**−**5e** readily produces the desired palladium complexes **6b**−**6e** (Scheme 3). Complexes **6c** and **6d** can be purified in the air via flash chromatography using ether/hexanes as the eluent.

Analysis of complexes **6a**−**6e** by ^{1}H NMR spectroscopy gives information about the solution structure. On the NHC ligand, the backbone protons on C4 and C5 of the imidazol-2-ylidene are equivalent, indicating either the presence of a mirror plane bisecting the NHC or a mechanism of exchange that is rapid on the NMR time scale. There are two septets for the methine protons of the isopropyl groups, indicating loss of the mirror plane that contains the imidazolylidene ring. Consistent with this loss of symmetry, there are three signals for the methyl protons on the isopropyl groups, with an intensity ratio of 6:6:12. These features are consistent with a chiral square-planar palladium complex with rapid rotation about the palladium−NHC bond. They also indicate that there is no rotation about the nitrogen−aryl bonds, the Pd−cinnamyl bonds, or the aryl−isopropyl bonds on the NMR time scale. The NMR spectra of **6b**−**6e** are very similar to those reported previously for **6a**.[12] The added trityl substituents in **6b**−**6d** are spinning rapidly around the C(2,6-diisopropylphenyl)−C(trityl) bond on the NMR time scale, as demonstrated by the equivalence of the protons on each aryl ring of the trityl substituents.

X-ray Crystal Structures. To accurately gauge the structural effects of the substituents on the NHC aryl rings, we report X-ray crystal structures of complexes **6b** (Figure 1) and **6c** (Figure 2). We have been unable to generate satisfactory crystals of complexes **6d** or **6e**. As substitutes, we describe the crystal structures of NHC·HBF_4 salts **4d** (Figure 3) and **4e** (Figure 4).

The cores of the complexes **6b** and **6c** closely resemble that of **6a**, which contained two crystallographically inequivalent

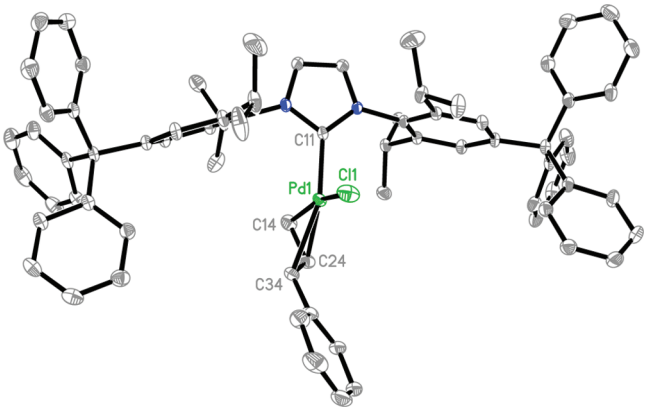

Figure 1. ORTEP diagram of complex **6b**, using 50% thermal ellipsoids. Hydrogen atoms are omitted for clarity.

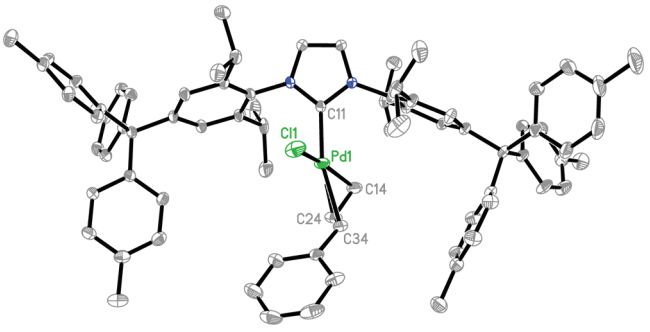

Figure 2. ORTEP diagram of complex **6c**, using 50% thermal ellipsoids. Hydrogen atoms are omitted for clarity.

molecules in the asymmetric unit.[12] In all three structures, the π-allyl group lies in the plane of the other coordinating atoms, taking up two coordination positions in the square-planar palladium(II) complex. The NHC ring is perpendicular to the Pd square plane, consistent with the proton NMR data presented above. Table 1 shows a comparison of the distances from palladium to the carbon atom of the NHC ligand, and also to the terminal (C14) and internal (C34) atoms of the allyl group within the cinnamyl ligand. None of these measures display any substantial differences between the different crystal structures **6a**−**6c**. Marion et al. used the difference between the Pd−C(allyl)

dx.doi.org/10.1021/om200349y |*Organometallics* 2011, 30, 5123–5132

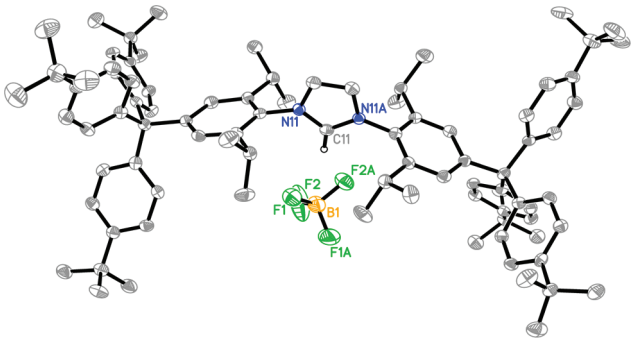

Figure 3. ORTEP diagram of imidazolium salt **4d**, using 50% thermal ellipsoids. Hydrogen atoms (except the imidazolium C−H) are omitted for clarity.

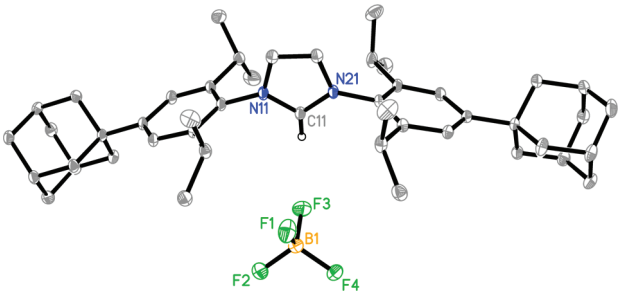

Figure 4. ORTEP diagram of imidazolium salt **4e**, using 50% thermal ellipsoids. Hydrogen atoms (except the imidazolium C−H) are omitted for clarity.

Table 1. Bond Distances (Å) in Literature Complex 6a and New Complexes

compound	Pd−NHC	Pd−C14	Pd−C34
6a	2.025(7)	2.125(7)	2.250(9)
	2.064(8)	2.136(10)	2.279(10)
6b	2.029(1)	2.08(1)	2.28(1)
6c	2.024(1)	2.11(2)	2.26(2)

distances as a measure of the trans-influence of the NHC, from which one could infer the relative ability to extrude the allyl group during activation of the catalyst.[12] Both **6b** and **6c** had disorder in the cinnamyl ligands, so the uncertainty in the Pd−C(allyl) distances is high and small differences might be obscured. However, one may still conclude that there is no evidence of *significant* conformational or electronic differences upon remote substitution of the NHC aryl groups.

Quantitative Steric Parameters. Assuming that the *para*-alkyl substituent on the aryl group of an NHC exerts a negligible electronic influence, the only significant source of differences comes from steric effects. To compare the ligand sterics to those in literature NHC ligands, it is necessary to calculate quantitative steric parameters $\%V_{bur}$ and G (defined below), which use the X-ray crystal structures of **6a** versus **6b** and **6c**. Because **6d** and **6e** were not crystallized, we compare HBF_4 salts **4d** and **4e** to known IPr·HX salts[17] in order to gauge the influence of para substituents for these ligands.

The percent buried volume ($\%V_{bur}$) is defined as the percent of the total volume of a sphere of radius 3.5 Å that is occupied by the ligand. Table 2 gives $\%V_{bur}$ values for the new ligands from

Table 2. Calculated $\%V_{bur}$ Values for IPr-Derived NHCs

compound	$\%V_{bur}$ values at distance		
	2.00 Å	2.10 Å	2.28 Å
6a#1	34.9	33.0	29.6
6a#2	36.7	34.9	31.6
6a (av)	35.8	34.0	30.6
6b	36.9	35.1	31.8
6c	40.0	38.2	35.0
$IPrH^+Cl^-$	47.3	45.3	41.8
$IPrH^+OTf^-$	43.6	41.7	38.3
$IPrH^+AlCl_4^-$	48.4	46.4	42.8
$IPrH^+$ (av)	46.4	44.5	41.0
4d#1	46.6	44.7	41.1
4d#2	47.2	45.3	41.7
4d (av)	46.9	45.0	41.4
4e	37.6	35.7	32.3

the crystal structures, calculated using the online tool Samb*V*ca.[18] This program normalizes the M−C distance to facilitate comparison of ligands, and there is no obvious choice of M−C distance to use. Thus, our calculations use three different M−C bond distances: 2.00, 2.10, and 2.28 Å. In cases where two crystallographically nonequivalent complexes or salts are present in the unit cell, results are reported for each independent molecule, and also as an average. The results are shown in Table 2. There are no consistent trends in the values according to the size of the substituent. In general, one also needs to bear in mind the low precision of calculated $\%V_{bur}$ values. For example, the range of $\%V_{bur}$ values for different complexes of the *same* IPr ligand ranges from 31.0 to 47.6 at 2.00 Å and from 26.0 to 42.1 at 2.28 Å,[11] and all of our new ligands fell within that range.

To test the influence of the distant substituent upon the calculated $\%V_{bur}$ values, we repeated the $\%V_{bur}$ calculations on truncated versions of complexes **6b** and **6c** and salts **4d** and **4e**, using identical crystallographic coordinates, but with the substituents at the 4′ positions of the 2,6-diisopropylphenyl groups manually deleted. For each ligand, the $\%V_{bur}$ values for the truncated ligand are identical to those for the nontruncated ligand, irrespective of the M−C bond distance chosen. This is not surprising, as the $\%V_{bur}$ measure considers only the buried volume within 3.5 Å of the metal, and the para substituents on the aryl groups are at least 6 Å from the metal. In sum, the differences in $\%V_{bur}$ values between the IPr variants presented here do not accurately reflect the sizes of the ligands (and, as we shall show below, the difference in catalytic reactivity).

Recent papers have introduced the use of solid angles as a quantitative steric measure.[19] These can be visualized by envisioning a light source at the metal, and a circumscribing sphere of radius r upon which this light may fall unless it is blocked by the ligand (Figure 5). The ligand casts a shadow upon an area A of the sphere, and the solid angle distended by the ligand is $\Omega = A/r^2$. (This differs from a cone angle in that the area A is not necessarily circular.) Because solid angle values are in the inconvenient units of steradians, it is preferable to divide Ω by 4π steradians (the solid angle of a complete sphere) to give a unitless value called percent coverage (G).[19] G represents the fraction of a hollow coordination sphere that is blocked by the ligand. For our calculations of G parameters for NHC ligands, M−C bond

dx.doi.org/10.1021/om200349y |*Organometallics* 2011, 30, 5123–5132

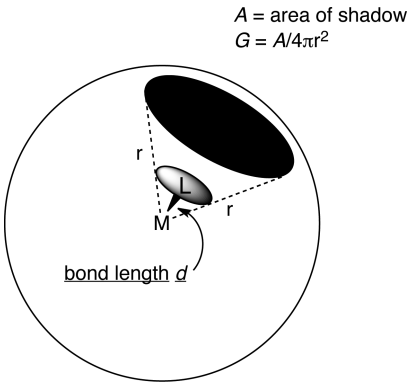

Figure 5. The *G* parameter for a ligand describes the fraction of a circumscribing sphere in the shadow of a ligand. Unlike a cone angle, the shadowed area is not necessarily circular, and therefore, "gearing" of ligands is taken into account.

Table 3. Calculated *G* Values[a] for IPr-Derived NHCs

compound	*G* (%) at distance *d*		
	2.00 Å	2.10 Å	2.28 Å
6a#1	42.3	41.2	39.1
6a#2	43.4	42.2	40.1
6b	49.2	48.0	46.1
6b (trunc.)[b]	42.5	41.1	39.1
6c	56.6	55.6	53.9
6c (trunc.)[b]	45.3	44.0	41.8
[IPrH]Cl[17]	48.1	46.7	44.4
[IPrH]OTf[21]	46.9	45.5	43.2
[IPrH]$AlCl_4$[22]	48.6	47.2	44.7
4d#1	58.7	57.4	55.3
4d#1 (trunc.)[b]	47.1	45.6	43.1
4d#2	57.6	56.5	54.5
4d#2 (trunc.)[b]	48.1	46.8	44.3
4e	47.4	46.3	44.3
4e (trunc.)[b]	43.9	42.7	40.6

[a] *G* is the fraction of the coordination sphere overshadowed by the ligand. See text and ref 19. [b] Truncated by deleting atoms from the trityl groups from the input file.

distances are again standardized for consistency, and *G* parameters using several M−C distances are shown in Table 3.[20] Values are also given for the Pd−NHC structures modified by artificial truncation at the 4′ position, as described above in the discussion on $\%V_{bur}$ values.

The *G* values reflect the increase of size due to the para substituents on the NHC aryl groups. The *G* values decrease markedly when the ligands are truncated, in contrast to the situation described above for the $\%V_{bur}$ values. This decrease upon truncation is about 4% for adamantyl-substituted **4e**, about 7% for the trityl-substituted **6b**, and 10−12% for larger trityl groups in **6c** and **4d**. This shows that the para substituents overshadow a part of the metal's coordination sphere that was not covered by the IPr ligand alone.

Suzuki−Miyaura Reactions. The Suzuki−Miyaura reaction is a powerful method for the formation of carbon−carbon bonds.[23] Although phosphines have typically been used as supporting ligands for palladium in Suzuki−Miyaura couplings,[2,24] IPr complex **6a** has been shown to be very active and robust as a precatalyst for this reaction, with catalyst loadings as low as 50 ppm, using technical grade isopropanol as a solvent.[12,25] It might seem difficult to improve upon this reaction, but, as shown below, the supersized versions of the catalyst are even more active.

Scheme 4. Suzuki−Miyaura Reaction under Soluble Conditions

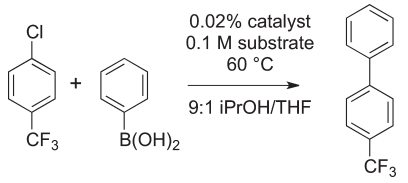

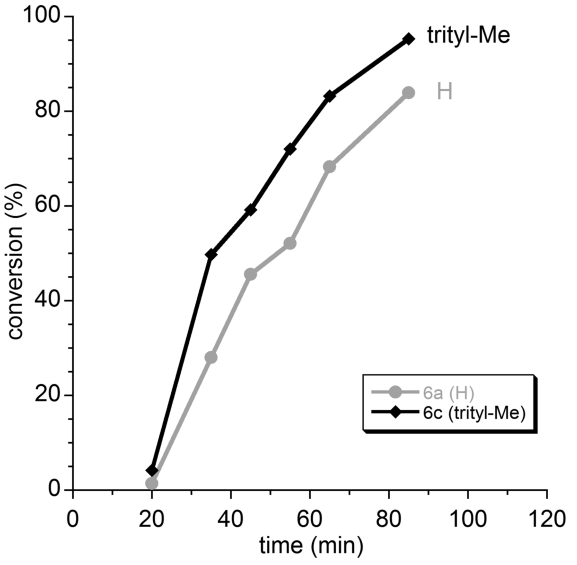

Figure 6. Plot of conversion versus time for the cross-coupling of *p*-chloro(trifluoromethyl)benzene with phenylboronic acid at 60 °C using a 100 ppm catalyst loading in ^{i}PrOH. Conversions measured using gas chromatography (see the Experimental Section).

We chose the reaction of *p*-chloro(trifluoromethyl)benzene and phenylboronic acid as a test reaction for study (Scheme 4). The conditions used by Nolan and co-workers with catalyst **6a**[12] provided an excellent starting point for a qualitative comparison to **6b**−**6e**. For an initial experiment, we compared the turnover number (TON) and turnover frequency (TOF) of one trityl-substituted catalyst (**6c**) to the parent catalyst **6a** at Nolan's conditions (^{i}PrOH, 60 °C, 100 ppm Pd), but at a halved substrate concentration to help improve solubility. Under these conditions, both catalysts **6a** and **6c** showed induction periods of ca. 20 min (Figure 6), and the trityl-substituted catalyst **6c** showed a slightly larger TON (19 000 in 85 min) and maximum TOF (36 000 h^{-1} measured between the 20 and 35 min time points) than parent catalyst **6a** (15 000 in 85 min, and 21 000 h^{-1}).

It is important to note that these conditions are not ideal for a fair comparison of catalysts. For example, the reaction is heterogeneous under the reported conditions (1 mmol of aryl halide in 1 mL of isopropanol), and it is important that differences in

dx.doi.org/10.1021/om200349y |*Organometallics* 2011, 30, 5123–5132

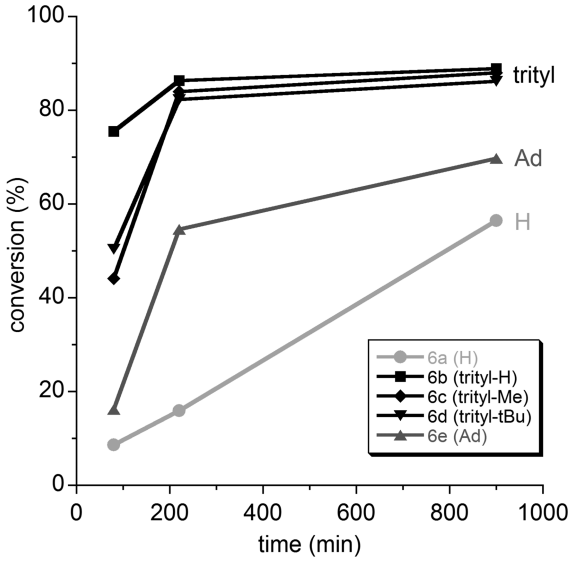

Figure 7. Plot of conversion versus time for the cross-coupling of *p*-chloro(trifluoromethyl)benzene with phenylboronic acid at 60 °C using a 0.02% catalyst loading in 9:1 ^{i}PrOH/THF. Conversions measured using gas chromatography (see the Experimental Section).

solubility should not influence the comparison of catalyst performance. Therefore, in subsequent experiments, the concentrations of aryl halide and boronic acid are reduced to 0.10 M and the solvent system is a 9:1 mixture of isopropanol and THF. A catalyst loading of 0.02% and a reaction temperature of 60 °C gives a rate at which complexes **6a**−**6e** may be more reliably compared (Figure 7). We reiterate that these conditions are optimized for catalyst comparison, not for conversion.

Under the modified conditions, it is clear that the catalysts **6b**−**6e**, which have NHCs with remote substitution, give a significant improvement in catalyst activity over the control catalyst **6a**. The rates roughly correlate with increased size as measured with the *G* value, which indicates that the adamantyl-substituted ligand covers a fraction of the coordination sphere that is intermediate between the aryl with no para substituent and the aryls with *para*-trityl groups. However, the predictive ability of the solid angle is limited: though the solid angles are larger for **6c** and **6d** due to the additional groups on the trityl substituents, the catalytic activity is not improved over the trityl-substituted **6b**. It is possible that the *G* values will have a greater ability to predict reactivity if they take ligand dynamics into account, as was done in recent reports of NHC complexes with flexible steric bulk.[26,27]

The new results reported here build on literature reports showing that bulky NHC ligands perform exceptionally well in Suzuki−Miyaura reactions.[28] The beneficial effects of larger supporting NHC ligands on the rate of the Suzuki−Miyaura reaction are typically understood as the ability of the bulkier ligand to stabilize monoligated Pd(0) intermediates.[12,24,29] However, previous studies have focused on introducing substituents very close to the metal center. The results described here show that substituents distant from the metal can also have a marked influence on catalytic rate. One potential explanation for the higher activity of the trityl-substituted NHC ligands is that the coordination of multiple NHC ligands (which would inhibit the reaction) is prevented by steric interactions between the trityl groups. Other influences of ligand size might also contribute to the observed rate increases. For example, the bulky substituents may inhibit aggregate formation. The differences in reactivity are probably not due to differences in the stability of the catalyst, because the overall final conversion of the Suzuki−Miyaura reaction is similar with all catalysts, including the less-active IPr complex **6a**.

CONCLUSIONS

The synthesis of substituted IPr derivatives and the derived π-cinnamylpalladium complexes reveals several interesting observations. The synthesis of 4-trityl derivatives of 2,6-diisopropylaniline is straightforward, as long as changes are implemented in the synthesis to account for changes in solubility. These exceptionally large NHC ligands are special additions to the growing number of bulky NHC ligands, which have many applications in catalysis. Using Suzuki−Miyaura coupling conditions that are modified for purposes of ligand comparison, it is clear that trityl-subsitituted NHC complexes **6b**−**6d** produce palladium catalysts that are significantly more active than the parent NHC ("IPr"). Though $\%V_{bur}$ is popular for measuring steric effects as a predictor of reactivity, it does not predict these changes in ligand sterics within this family of IPr derivatives. This is because $\%V_{bur}$ is influenced only by bulk close to a metal, though more distant substituents can also have an important influence. *G* parameters derived from solid angles are more effective in predicting the changes in size and roughly correlate with the increase in catalytic activity.

EXPERIMENTAL SECTION

General Considerations. Unless otherwise noted, reactions were performed under nitrogen. Tris(4-methylphenyl)methanol **1c**,[30] tris(4-*tert*-butylphenyl)methanol **1d**,[31] 4-(1′-adamantyl)-2,6-diisopropylaniline **2e**,[32] [(π-cinnamyl)PdCl]$_2$,[12] and Pd complex **6a**[12] were prepared according to published procedures. Potassium *tert*-butoxide was purchased from Aldrich and purified via sublimation. 2,6-Diisopropylaniline was purchased from TCI or Acros and purified by vacuum distillation prior to use. *p*-Chloro(trifluoromethyl)benzene was purified by distillation under nitrogen. Phenylboronic acid was purified via flash chromatography using 2:1 ethyl acetate/hexanes.[33,34] It is critical to purify the phenylboronic acid prior to use in order to obtain reproducible solubility in Suzuki−Miyaura coupling reactions. Isopropanol and THF were degassed via nitrogen sparge for a minimum of 30 min before use in Suzuki−Miyaura coupling experiments.

Aniline 2b. To a 500 mL Schlenk flask equipped with a stir bar was added glacial acetic acid (150 mL), followed by triphenylmethanol **1b** (26.0 g, 100 mmol). The flask was then fitted with a rubber septum, and the contents were sparged with nitrogen for ca. 15 min. 2,6-Diisopropylaniline **2a** (28 mL, 150 mmol) was then added via a syringe, followed by concentrated HCl (9.1 mL, 110 mmol). The flask was then heated in an 80 °C oil bath overnight, under an inert atmosphere. The reaction mixture was then allowed to cool to room temperature. The resulting solid was isolated via filtration and washed with water, followed by methanol, and dried under vacuum. Crystallization from hot ethanol yielded **2b** as a white solid (31.9 g, 76% yield). ^{1}HNMR (400 MHz, $CDCl_3$): δ 1.09 (d, J = 6.9 Hz, 12H, $CHMe_2$), 2.87 (septet, J = 6.9 Hz, 2H, $CHMe_2$), 3.65 (br s, 2H, NH_2), 6.83 (s, 2H, Ar*H*), 7.15−7.26 (m, 15H, Ar*H*) ppm. $^{13}C\{^{1}H\}$ NMR (101.6 MHz, $CDCl_3$): δ 22.46, 27.97, 64.80, 125.55, 126.05, 127.15, 131.18, 136.42, 137.69, 147.55 ppm. Anal. Calcd for $C_{31}H_{33}N$: C, 88.73; H, 7.93; N, 3.34. Found: C, 88.70; H, 8.07; N, 3.68.

Aniline 2c. To a 500 mL flask equipped with a stir bar was added glacial acetic acid (190 mL), followed by tris-(4-methylphenyl)methanol **1c** (19.62 g, 64.9 mmol). The flask was then fitted with a rubber septum and the contents sparged with nitrogen for ca. 15 min. 2,6-Diisopropylaniline **2a** (18.4 mL, 97.3 mmol) was then added via a syringe, followed by concentrated HCl (5.9 mL, 71 mmol). The flask was then heated in an 80 °C oil bath for 8 h, under an inert atmosphere. The reaction mixture was then allowed to cool to room temperature. A 2 M solution of aqueous KOH (ca. 75 mL) was then slowly added to the reaction mixture. The resulting solid was isolated via filtration and washed with water, followed by methanol, and dried under vacuum to yield **2c** as a white solid (27.8 g, 92.7% yield). ^{1}HNMR (400 MHz, $CDCl_3$): δ 1.11 (d, J = 6.5 Hz, 12H, CHMe_2), 2.31 (s, 9H, ArMe), 2.88 (septet, J = 6.8 Hz, 2H, CHMe$_2$), 3.65 (br s, 2H, NH_2), 6.87 (s, 2H, ArH), 7.02 (d, 6H, J = 8.0 Hz, ArH), 7.12 (d, 6H, J = 8.0 Hz, ArH) ppm. ^{13}C{^{1}H} NMR (101.6 MHz, $CDCl_3$): δ 20.85, 22.46, 27.97, 63.74, 125.88, 127.79, 130.87, 131.14, 134.66, 136.93, 137.35, 144.93 ppm. Anal. Calcd for $C_{34}H_{39}N$: C, 88.45; H, 8.51; N, 3.03. Found: C, 88.19; H, 8.57; N, 3.10.

Aniline 2d. To a 500 mL Schlenk flask equipped with a stir bar was added glacial acetic acid (220 mL), followed by tris-(4-tert-butylphenyl)-methanol **1d** (15.58 g, 36.3 mmol). The flask was then fitted with a rubber septum and the contents sparged with nitrogen for ca. 15 min. 2,6-Diisopropylaniline **2a** (10.3 mL, 54.4 mmol) was then added via a syringe, followed by concentrated HCl (3.3 mL, 40 mmol). The flask was then heated in an 80 °C oil bath for 8 h, under an inert atmosphere. The reaction mixture was then allowed to cool to room temperature, then 2 M aqueous KOH (ca. 40 mL) was slowly added to the reaction mixture. The resulting solid was isolated via filtration and washed with water, followed by methanol, and dried under vacuum to yield **2d** as a white solid (20.6 g, 96.7% yield). ^{1}H NMR (400 MHz, $CDCl_3$): δ 1.08 (d, J = 6.9 Hz, 12H, CHMe_2), 1.30 (s, 27H, CMe_3), 2.86 (septet, J = 6.9 Hz, 2H, CHMe$_2$), 3.62 (br s, 2H, NH_2), 6.74 (s, 2H, ArH), 7.11 (d, 6H, J = 8.5 Hz, ArH), 7.22 (d, 6H, J = 8.5 Hz, ArH) ppm. ^{13}C{^{1}H} NMR (101.6 MHz, $CDCl_3$): δ 22.42, 27.97, 31.40, 34.25, 63.52, 123.74, 126.18, 130.86, 137.17, 137.45, 144.60, 148.04 ppm. Anal. Calcd for $C_{43}H_{57}N$: C, 87.85; H, 9.77; N, 2.38. Found: C, 87.83; H, 9.85; N, 2.42.

α-Diimine 3b. To a 500 mL flask equipped with a stir bar was added aniline **2b** (13.1 g, 31.2 mmol), followed by ethanol (225 mL), in air. The flask was then fitted with a condenser and heated with an 80 °C oil bath. After most of the material had dissolved, aqueous glyoxal (1.8 mL, 16 mmol) was added to the flask, followed by formic acid (2 drops). The reaction mixture immediately began to develop a yellow color, followed by the precipitation of a yellow solid. The flask was heated at 80 °C for 4 h and then allowed to cool to room temperature. The resulting solid was isolated via filtration, washed with methanol, and dried under vacuum to yield impure **3b** as a yellow powder (12.0 g, 89.2% yield). ^{1}HNMR (400 MHz, $CDCl_3$): δ 1.03 (d, J = 6.8 Hz, 24H, CHMe_2), 2.89 (septet, J = 6.8 Hz, 4H, CHMe$_2$), 7.00 (s, 4H, ArH), 7.15−7.29 (m, 30H, ArH), 8.12 (s, 2H, ArN=CH) ppm.

α-Diimine 3c. To a 250 mL flask equipped with a stir bar was added aniline **2c** (4.62 g, 10.0 mmol), followed by ethanol (90 mL), in air. The flask was then fitted with a condenser and heated with an 80 °C oil bath. After most of the material dissolved, aqueous glyoxal (0.57 mL, 5.0 mmol) was added to the flask, followed by formic acid (1 drop). The reaction mixture immediately began to develop a yellow color, followed by the precipitation of a yellow solid. The flask was heated at 80 °C for 4 h and then allowed to cool to room temperature. The resulting solid was isolated via filtration, washed with methanol, and dried under vacuum to yield impure **3c** as a yellow powder (4.69 g, 99.1% yield). ^{1}H NMR (400 MHz, $CDCl_3$): δ 1.27 (d, J = 6.8 Hz, 24H, CHMe_2), 2.56 (s, 18H, ArMe), 3.12 (septet, J = 6.8 Hz, 4H, CHMe$_2$), 7.29 (d, 12H, J = 8.8 Hz, ArH), 7.37 (d, 12H, J = 8.8 Hz, ArH), 7.51 (s, 4H, ArH), 8.35 (s, 2H, ArN=CH) ppm.

α-Diimine 3d. To a 100 mL flask equipped with a stir bar was added aniline **2d** (3.02 g, 5.13 mmol), followed by ethanol (45 mL), in air. The flask was then fitted with a condenser and heated with an 80 °C oil bath. After most of the material dissolved, aqueous glyoxal (0.29 mL, 2.6 mmol) was added to the flask, followed by formic acid (1 drop). The reaction mixture immediately began to develop a yellow color, followed by the precipitation of a yellow solid. The flask was heated at 80 °C for 4 h and then allowed to cool to room temperature. The resulting solid was isolated via filtration and washed with methanol and dried under vacuum to yield impure **3d** as a yellow powder (2.78 g, 90.3% yield). ^{1}H NMR (400 MHz, $CDCl_3$): δ 1.00 (d, J = 6.8 Hz, 24H, CHMe_2), 1.31 (s, 54H, CMe_3), 2.87 (septet, J = 6.9 Hz, 4H, CHMe$_2$), 6.88 (s, 2H, ArH), 7.11 (d, 12H, J = 8.5 Hz, ArH), 7.25 (d, 12H, J = 8.5 Hz, ArH), 8.10 (s, 2H, ArN=CH) ppm.

α-Diimine 3e. To a 250 mL flask equipped with a stir bar was added aniline **2e** (7.29 g, 23.4 mmol), followed by ethanol (100 mL), under air. The flask was then heated with a heat gun until all solids dissolved. Aqueous glyoxal (1.3 mL, 12 mmol) was then added to the flask, followed by formic acid (2 drops). The reaction mixture immediately began to develop a yellow color, followed by the precipitation of a yellow solid. The mixture was stirred at room temperature for 10 h. The resulting solid was isolated via filtration, washed with methanol, and dried under vacuum to yield impure **3e** as a yellow powder (5.56 g, 73.6% yield). ^{1}H NMR (400 MHz, $CDCl_3$): δ 1.21 (d, J = 7.0 Hz, 24H, CHMe_2), 1.80 (br s, 12H, AdH), 1.96 (br s, 12H, AdH), 2.12 (br s, 6H, AdH), 2.96 (septet, J = 6.7 Hz, 4H, CHMe$_2$), 7.17 (s, 2H, ArH), 8.11 (s, 2H, ArN=CH) ppm.

Imidazolium Tetrafluoroborate 4b. Yellow solid **3b** (12.0 g, 13.9 mmol) was added to a 250 mL flask with a stir bar, followed by paraformaldehyde powder (417 mg, 13.9 mmol), followed by toluene (100 mL), under air. The flask was then briefly heated to dissolve most of the solids and allowed to cool back to room temperature. After cooling, $HBF_4 \cdot Et_2O$ (2.8 mL, 21 mmol) was slowly added to the reaction mixture, allowing each drop of acid to fully disperse before adding another drop, with a total addition time of ca. 1 h. The reaction mixture was stirred at room temperature overnight. The resulting solid was isolated by filtration, washed with ether, and was purified by recrystallization from hot benzene to yield imidazolium tetrafluoroborate **4b** as a white solid (4.67 g, 35.0% yield). ^{1}H NMR (400 MHz, $CDCl_3$): δ 1.06 (d, J = 6.7 Hz, 12H, CHMe_2), 1.10 (d, J = 7.0 Hz, 12H, CHMe_2), 2.87 (m, 4H, CHMe$_2$), 7.22−7.35 (m, 30H, ArH),7.88 (s, 2H, RNCHCHNR), 8.71 (s, 1H, RNCHNR) ppm. ^{13}C{^{1}H} NMR (101.6 MHz, $CDCl_3$): δ 23.53, 24.18, 28.98, 65.32, 126.23, 126.73, 127.18, 127.67, 127.73, 130.89, 136.83, 143.58, 145.92, 151.27 ppm. Anal. Calcd for $C_{65}H_{65}BF_4N_2$: C, 81.24; H, 6.82; N, 2.91. Found: C, 81.17; H, 6.74; N, 2.96.

Imidazolium Tetrafluoroborate 4c. Yellow solid **3c** (4.69 g, 4.96 mmol) was added to a 100 mL flask with a stir bar, followed by paraformaldehyde powder (190 mg, 6.2 mmol), followed by toluene (50 mL), under air. The flask was then briefly heated with a heat gun to dissolve most of the solids and allowed to cool back to room temperature. After cooling, $HBF_4 \cdot Et_2O$ (1.0 mL, 7.4 mmol) was slowly added to the reaction mixture, allowing each drop of acid to fully disperse before adding another drop, with a total addition time of ca. 30 min. The reaction stirred at room temperature overnight. The reaction was then quenched by the dropwise addition of aqueous sodium bicarbonate (ca. 5 mL). The resulting solid was isolated by filtration and was purified by recrystallization from hot benzene to yield imidazolium tetrafluoroborate **4c** as a white solid (1.45 g, 28.0% yield). ^{1}HNMR (400 MHz, $CDCl_3$): δ 1.00 (d, J = 6.8 Hz, 12H, CHMe_2), 1.10 (d, J = 6.8 Hz, 12H, CHMe_2), 2.29−2.37 (m, 22H, ArMe and CHMe$_2$), 7.07 (d, J = 8.8 Hz, 12H, ArH), 7.12 (d, J = 8.8 Hz, 12H, ArH), 7.25 (s, 4H, ArH), 7.94 (s, 2H, J = 8.0 Hz, RNCHCHNR), 8.36 (s, 1H, RNCHNR) ppm. ^{13}C{^{1}H} NMR (101.6 MHz, $CDCl_3$): δ 20.85, 23.55, 24.31, 28.98,

64.36, 126.84, 127.11, 127.57, 128.38, 130.58, 130.67, 135.40, 135.58, 136.13, 143.30, 151.87 ppm. Anal. Calcd for $C_{71}H_{77}BF_4N_2$: C, 81.59; H, 7.43; N, 2.68. Found: C, 81.82; H, 7.41; N, 2.79.

Imidazolium Tetrafluoroborate 4d. Yellow solid **4d** (2.71 g, 2.26 mmol) was added to a 50 mL flask with a stir bar, followed by paraformaldehyde powder (68.0 mg, 2.26 mmol), followed by toluene (25 mL), under air. The flask was then briefly heated with a heat gun to dissolve most of the solids and allowed to cool back to room temperature. After cooling, $HBF_4 \cdot Et_2O$ (0.5 mL, 3 mmol) was slowly added to the reaction mixture, allowing each drop of acid to fully disperse before adding another drop, with a total addition time of ca. 30 min. The reaction stirred at room temperature overnight. The reaction was then quenched by the dropwise addition of aqueous sodium bicarbonate (ca. 3 mL). The resulting solid was isolated by filtration and was purified by recrystallization from hot benzene to yield imidazolium tetrafluoroborate **4d** as a white solid (1.04 g, 35% yield). ^{1}HNMR (400 MHz, $CDCl_3$): δ 0.97 (d, J = 6.8 Hz, 12H, CHMe_2), 1.08 (d, J = 6.8 Hz, 12H, CHMe_2), 1.30 (s, 54H, CMe_3), 2.34 (septet, J = 6.8 Hz, 4H, CHMe$_2$), 7.09 (d, 12H, J = 8.8 Hz, ArH), 7.12 (s, 4H, ArH), 7.28 (d, 12H, J = 8.8 Hz, ArH), 8.00 (s, 2H, RNCHCHNR), 8.28 (s, 1H, RNCHNR) ppm. $^{13}C\{^1H\}$ NMR (101.6 MHz, $CDCl_3$): δ 23.44, 24.29, 28.90, 31.27, 34.31, 64.03, 123.92, 124.30, 127.87, 128.15, 130.57, 141.22, 142.86, 143.17, 148.95, 149.40 ppm. Anal. Calcd for $C_{89}H_{113}BF_4N_2$: C, 82.37; H, 8.78; N, 2.16. Found: C, 82.39; H, 8.70; N, 2.08.

Imidazolium Tetrafluoroborate 4e. Yellow solid **3e** (5.55 g, 8.61 mmol) was added to a 50 mL flask with a stir bar, followed by paraformaldehyde powder (259 mg, 8.61 mmol), followed by toluene (20 mL). The flask was then briefly heated with a heat gun to dissolve most of the solids and allowed to cool back to room temperature. After cooling, $HBF_4 \cdot Et_2O$ (1.5 mL, 11 mmol) was slowly added to the reaction mixture, allowing each drop of acid to fully disperse before adding another drop, with a total addition time of ca. 30 min. The reaction was stirred at room temperature overnight. The resulting solid was isolated by filtration, washed with ether, and was purified by recrystallization from acetone/ether to yield imidazolium tetrafluoroborate **4e** as a tan solid (1.30 g, 20.0% yield). ^{1}H NMR (400 MHz, $CDCl_3$): δ 1.18 (d, J = 7.0 Hz, 12H, CHMe_2), 1.28 (d, J = 6.5 Hz, 12H, CHMe_2), 1.80 (dd, J = 12.5 and 7.0 Hz, 12H, AdH), 1.94 (br s, 12H, AdH), 2.14 (br s, 6H, AdH), 2.41 (septet, J = 7.0 Hz,4H, CHMe$_2$), 7.30 (s, 4H, ArH), 7.82 (s, 2H, RNCHCHNR), 8.38 (s, 1H, RNCHNR) ppm. $^{13}C\{^1H\}$ NMR (101.6 MHz, $CDCl_3$): δ 23.82, 24.55, 28.74, 29.14, 36.54, 36.80, 42.91, 121.22, 126.96, 127.11, 136.28, 144.16, 155.37 ppm. Anal. Calcd for $C_{47}H_{65}BF_4N_2$: C, 75.79; H, 8.80; N, 3.76. Found: C, 75.73; H, 8.79; N, 4.06.

NHC 5b. In a N_2-filled glovebox, a scintillation vial was charged with **4b** (0.48 g, 0.50 mmol), potassium *tert*-butoxide (56 mg, 0.50 mmol), and a stir bar, followed by toluene (ca. 5 mL). The resulting mixture was stirred overnight. The volatile materials were removed under vacuum. The resulting solid was extracted with a 1:4 mixture of toluene and benzene (ca. 5 mL) and then filtered through Celite. The solids were washed with 2 × 1 mL portions of benzene, and the combined filtrate was evaporated under vacuum to yield NHC **5b** as a white solid (407 mg, 93% yield). ^{1}H NMR (400 MHz, C_6D_6): δ 1.06 (d, J = 6.5 Hz, 12H, CHMe_2), 1.25 (d, J = 6.5 Hz, 12H, CHMe_2), 2.95 (septet, J = 6.9 Hz, 4H, CHMe$_2$), 6.53 (s, 2H, RNCHCHNR), 6.95−7.05 (m, 6H, ArH), 7.07−7.12 (m, 12H, ArH), 7.45 (s, 4H, ArH), 7.46−7.51 (m, 12H, ArH) ppm. $^{13}C\{^1H\}$ NMR (101.6 MHz, C_6D_6): δ 23.22, 24.40, 28.60, 65.64, 121.28, 126.05, 126.76, 129.02, 131.36, 136.43, 144.80, 147.12, 219.95 ppm. Anal. Calcd for $C_{65}H_{64}N_2$: C, 89.40; H, 7.39; N, 3.21. Found: C, 88.82; H, 7.48; N, 3.44.

NHC 5c. In the glovebox, a scintillation vial was charged with a stir bar, **5c** (520 mg, 0.50 mmol), and potassium *tert*-butoxide (62 mg, 0.55 mmol), followed by toluene (ca. 5 mL). The resulting mixture was stirred overnight. The volatile materials were removed under vacuum. The resulting solid was extracted with a 1:4 mixture of toluene and benzene (ca. 5 mL) and then filtered through Celite. The solids were washed with 2 × 1 mL portions of benzene, and the combined filtrate was evaporated under vacuum to yield NHC **5c** as a white solid (480 mg, >99% yield). ^{1}H NMR (400 MHz, C_6D_6): δ 1.10 (d, J = 6.9 Hz, 12H, CHMe_2), 1.29 (d, J = 6.9 Hz, 12H, CHMe_2), 2.07 (s, 18H, ArMe), 2.98 (septet, J = 6.9 Hz, 4H, CHMe$_2$), 6.54 (s, 2H, RNCHCHNR), 6.97 (d, J = 8.0 Hz, 12H, ArH), 7.51 (d, J = 8.0 Hz, 12H, ArH), 7.58 (s, 4H, ArH) ppm. $^{13}C\{^1H\}$ NMR (101.6 MHz, C_6D_6): δ 20.55, 23.26, 24.49, 28.65, 64.81, 121.29, 125.38, 126.63, 129.01, 131.21, 135.18, 136.35, 144.72, 147.65, 220.34 ppm. Anal. Calcd for $C_{71}H_{76}N_2$: C, 89.07; H, 8.00; N, 2.93. Found: C, 87.58; H, 8.28; N, 3.14.

NHC 5d. In the glovebox, a scintillation vial was charged with a stir bar, **4d** (324 mg, 0.250 mmol), and potassium *tert*-butoxide (31.0 mg, 0.275 mmol), followed by toluene (ca. 3 mL). The resulting mixture was stirred overnight. The volatile materials were removed under vacuum. The resulting solid was extracted with a 1:4 mixture of toluene and benzene (ca. 5 mL) and then filtered through Celite. The solids were washed with 2 × 1 mL portions of benzene, and the combined filtrate was concentrated under vacuum to yield NHC **5d** as a white solid (300 mg, >99% yield). ^{1}H NMR (400 MHz, C_6D_6): δ 1.08 (d, J = 7.0 Hz, 12H, CHMe_2), 1.20 (s, 54H, CMe_3), 1.28 (d, J = 6.5 Hz, 12H, CHMe_2), 2.99 (septet, J = 6.8 Hz, 4H, CHMe$_2$), 6.56 (s, 2H, RNCHCHNR), 7.21 (d, 12H, J = 8.5 Hz, ArH), 7.50 (s, 4H, ArH), 7.53 (d, 12H, J = 8.5 Hz, ArH) ppm. $^{13}C\{^1H\}$ NMR (101.6 MHz, C_6D_6): δ 23.14, 24.48, 28.64, 31.14, 34.05, 64.56, 121.28, 124.40, 125.38, 131.26, 136.43, 144.55, 147.69, 148.44, 220.35 ppm. Anal. Calcd for $C_{89}H_{112}N_2$: C, 88.35; H, 9.33; N, 2.32. Found: C, 87.34; H, 8.96; N, 2.28.

NHC 5e. In the glovebox, a scintillation vial equipped with a stir bar was charged with **4e** (0.37 g, 0.50 mmol) and potassium *tert*-butoxide (56 mg, 0.50 mmol), followed by toluene (ca. 5 mL). The resulting mixture was stirred overnight. The volatile materials were removed under vacuum. The resulting solid was extracted with a 1:4 mixture of toluene and benzene (ca. 5 mL) and then filtered through Celite. The solids were washed with 2 × 1 mL portions of benzene, and the combined filtrate was evaporated under vacuum to yield NHC **5e** as a white solid (258 mg, 78% yield). ^{1}H NMR (400 MHz, C_6D_6): δ 1.32 (d, J = 7.0 Hz, 12H, CHMe_2), 1.39 (d, J = 7.0 Hz, 12H, CHMe_2), 1.73 (m, 12H, AdH), 2.04 (m, 18H, AdH), 3.08 (septet, J = 7.0 Hz, 4H, CHMe$_2$), 6.67 (s, 2H, RNCHCHNR), 7.45 (s, 4H, ArH) ppm. $^{13}C\{^1H\}$ NMR (101.6 MHz, C_6D_6): δ 23.56, 24.72, 28.83, 29.16, 36.57, 36.80, 43.39, 119.76, 121.38, 136.57, 145.32, 151.25, 220.27 ppm. Anal. Calcd for $C_{47}H_{64}N_2$: C, 85.92; H, 9.82; N, 4.26. Found: C, 86.25; H, 9.82; N, 4.56.

Complex 6b. In the glovebox, a scintillation vial was charged with [(cinnamyl)PdCl]$_2$ (62 mg, 0.12 mmol) and NHC **5b** (210 mg, 0.24 mmol), a stir bar, and toluene (ca. 3 mL). The reaction mixture stirred overnight and was then removed from the glovebox. The solvent was removed under vacuum, and the resulting solid was extracted with benzene. The mixture was filtered through Celite and dried under vacuum to yield **6b** as a tan solid (265 mg, 98% yield). ^{1}H NMR (400 MHz, C_6D_6): δ 0.99 (d, J = 6.5 Hz, 12H, CHMe_2), 1.31 (d, J = 6.5 Hz, 6H, CHMe_2), 1.37 (d, J = 6.5 Hz, 6H, CHMe_2), 1.87 (d, J = 11 Hz, 1H, cinnamyl$H$), 3.01 (d, J = 6.5 Hz, 1H, cinnamyl$H$), 3.13 (sept, J = 6.5 Hz, 2H, CHMe$_2$), 3.26 (septet, J = 6.5 Hz, 2H, CHMe$_2$), 4.46 (d, J = 13 Hz, 1H, cinnamyl$H$), 5.14−5.21 (m, 1H, cinnamyl$H$), 6.65 (s, 2H, RNCHCHNR), 6.93−7.00 (m, 6H, ArH), 7.01−7.05 (m, 1H, ArH), 7.07−7.11 (m, 12H, ArH), 7.21−7.26 (m, 2H, ArH), 7.40−7.48 (m, 16H, ArH) ppm. $^{13}C\{^1H\}$ NMR (101.6 MHz, $CDCl_3$): δ 22.61, 25.86, 28.47, 46.63, 65.31, 89.24, 108.97, 124.01, 125.93, 126.55, 126.80, 127.35, 127.47, 128.23, 131.06, 133.53, 138.23, 144.71, 146.62, 147.96, 185.29 ppm. Anal. Calcd for $C_{74}H_{73}ClN_2Pd$: C, 78.50; H, 6.50; N, 2.47. Found: C, 78.43; H, 6.41; N, 2.61.

Complex 6c. In the glovebox, a scintillation vial was charged with [(cinnamyl)PdCl]$_2$ (130 mg, 0.25 mmol), NHC **5c** (480 mg, 0.50 mmol),

a stir bar, and toluene (ca. 3 mL). The reaction was stirred for 4 h and was then removed from the glovebox. The reaction mixture was loaded directly onto a 25 mm column containing ca. 50 mL silica. The column was initially eluted with hexanes (ca. 75 mL) to immobilize all colored bands and then eluted with 10% ether in hexanes (v/v) until the first yellow band was collected. The yellow fractions were combined, concentrated, and dried under vacuum to yield **6c** as a tan solid (401 mg, 66% yield). ^{1}H NMR (400 MHz, C_6D_6): δ 0.99 (d, J = 6.0 Hz, 12H, CHMe_2), 1.33 (d, J = 6.5 Hz, 6H, CHMe_2), 1.39 (d, J = 6.0 Hz, 6H, CHMe_2), 2.07 (s, 18H, ArMe), 2.11 (d, J = 2 Hz, 1H, cinnamyl$H$), 3.01 (d, J = 6.0 Hz, 1H, cinnamyl$H$), 3.14 (m, 2H, CHMe$_2$), 3.26 (m, 2H, CHMe$_2$), 4.41 (d, J = 13 Hz, 1H, cinnamyl$H$), 5.09−5.17 (m, 1H, cinnamyl$H$), 6.64 (s, 2H, RNCHCHNR), 6.98 (d, J = 8.0 Hz, 12H, ArH), 7.01−7.25 (m, 5H, ArH), 7.66 (d, J = 8.0 Hz, 12H, ArH), 7.56 (s, 4H, ArH). ^{13}C{^{1}H} NMR (101.6 MHz, $CDCl_3$): δ 20.86, 22.62, 25.88, 28.47, 46.64, 64.34, 89.10, 108.95, 123.98, 126.46, 127.31, 128.02, 128.99, 130.91, 133.37, 135.14, 144.07, 144.52, 148.36, 185.33. Anal. Calcd for $C_{80}H_{85}ClN_2Pd$: C, 78.99; H, 7.04; N, 2.30. Found: C, 79.24; H, 7.03; N, 2.21.

Complex 6d. In the glovebox, a scintillation vial was charged with [(cinnamyl)PdCl]$_2$ (64.8 mg, 0.125 mmol) and NHC **5d** (300 mg, 0.250 mmol), a stir bar, and toluene (ca. 2 mL). The reaction was stirred for 3 h and was then removed from the glovebox. The reaction mixture was loaded directly onto a 25 mm column containing ca. 40 mL silica. The column was initially eluted with hexanes (ca. 75 mL) to immobilize all colored bands and then eluted with 10% ether in hexanes (v/v) until the first yellow band was collected. The yellow fractions were combined, concentrated, and dried under vacuum to yield **6d** as a tan solid (300 mg, 81.7% yield) ^{1}H NMR (400 MHz, C_6D_6): δ 0.99 (br s, 12H, CHMe_2), 1.19 (s, 54H, CMe_3), 1.27−1.39 (m, 12H, CHMe_2), 1.92 (d, J = 10 Hz, 1H, cinnamyl$H$), 3.01 (d, J = 5.5 Hz, 1H, cinnamyl$H$), 2.98−3.32 (m, 4H, CHMe$_2$), 4.45 (d, J = 13 Hz, 1H, cinnamyl$H$), 5.11−5.23 (m, 1H, cinnamyl$H$), 6.66 (s, 2H, RNCHCHNR), 7.23 (d, J = 8.5 Hz, 12H, ArH), 7.29 (d, J = 7.0 Hz, 2H, ArH), 7.52 (d, J = 8.5 Hz, 15H, ArH). ^{13}C{^{1}H} NMR (101.6 MHz, $CDCl_3$): δ 22.61, 25.86, 28.39, 31.32, 34.27, 46.76, 64.02, 88.95, 109.20, 124.02, 126.44, 126.95, 127.39, 128.17, 128.98, 130.74, 133.39, 143.69, 144.24, 148.49, 185.41. Anal. Calcd for $C_{98}H_{121}ClN_2Pd$: C, 80.13; H, 8.30; N, 1.91. Found: C, 80.22; H, 8.54; N, 2.06.

Complex 6e. In the glovebox, a scintillation vial equipped with a stir bar was charged with [(cinnamyl)PdCl]$_2$ (41 mg, 0.078 mmol) and NHC **5e** (103 mg, 0.16 mmol), followed by toluene (ca. 2 mL). The reaction mixture stirred overnight and was then removed from the glovebox. The solvent was removed under vacuum and the resulting solid extracted with benzene. The mixture was filtered through Celite and dried under vacuum to yield **6e** as a tan solid (135 mg, 94% yield). ^{1}H NMR (400 MHz, C_6D_6): δ 1.09−1.21 (m, 12H), 1.48−1.70 (m, 24H), 1.89−2.00 (m, 22H), 3.16 (d, J = 6.5 Hz, 1H, cinnamyl$H$), 3.31 (septet, J = 6.5 Hz, 2H, CHMe$_2$), 3.42 (septet, J = 7.0 Hz, 2H, CHMe$_2$), 4.21 (d, J = 12.5 Hz, 1H, cinnamyl$H$), 4.99−5.09 (m, 1H, cinnamyl$H$), 6.68 (s, 2H, RNCHCHNR), 6.91−7.00 (m, 3H, ArH), 7.05−7.11 (m, 2H, ArH), 7.44 (s, 4H, ArH). ^{13}C{^{1}H} NMR (101.6 MHz, $CDCl_3$): δ 22.60, 26.24, 28.62, 28.95, 31.54, 36.77, 43.18, 47.49, 87.73, 108.97, 120.04, 124.23, 126.38, 127.25, 128.08, 133.50, 138.43, 145.22, 152.35, 185.45. Anal. Calcd for $C_{56}H_{73}ClN_2Pd$: C, 73.42; H, 8.03; N, 3.06. Found: C, 73.63; H, 7.70; N, 2.88.

Suzuki Reactions. As noted above, it is critical to purify commercial phenylboronic acid by flash chromatography in order to obtain reproducible solubility. A 5 mL volumetric flask was charged with phenylboronic acid (71.1 mg, 0.583 mmol) and potassium *tert*-butoxide (68.6 mg, 0.611 mmol). The volumetric flask was then capped with a rubber septum and sparged with nitrogen for ca. 10 min. The solids were then dissolved in isopropanol, and the solution was diluted to 5.0 mL. A 1 mL volumetric flask was capped with a rubber septum and sparged with nitrogen for ca. 5 min. Mesitylene (139 μL, 1.00 mmol) and *p*-chloro-(trifluoromethyl)benzene (267 μL, 2.00 mmol) were then added to the 1 mL volumetric flask via a syringe. The liquids were then dissolved in THF, and the solution was diluted to 1.0 mL. Catalyst stock solutions were prepared at a concentration of 0.40 mM by first preparing stock solutions at a concentration of 4 mM and then performing 1/10 dilutions.

Each reaction was performed in a 1 dram vial containing a flea stir bar and capped with a septum cap. Each vial was sparged with nitrogen for ca. 5 min prior to use. To each vial was added 900 μL of the phenylboronic acid stock solution and 50 μL of the aryl halide stock solution. Each vial was then heated using an aluminum block heater set to 60 °C. After thermal equilibration, each reaction was initiated via the addition of 50 μL of the appropriate 0.40 mM catalyst solution, for a final palladium concentration of 20 μM. Aliquots (100 μL) were removed at reaction times of 80, 220, and 900 min. Aliquots were purified by filtration through pipet filters containing ca. 1 cm of silica and eluted with 1−1.2 mL of ethyl acetate directly into GC vials. Conversion was determined by comparison of the GC responses of product and the internal mesitylene standard.

■ ASSOCIATED CONTENT

Supporting Information. Crystallographic details. This material is available free of charge via the Internet at http://pubs.acs.org.

■ AUTHOR INFORMATION

Corresponding Author
*E-mail: holland@chem.rochester.edu.

■ ACKNOWLEDGMENT

This research was supported by the U.S. Department of Energy, Office of Basic Energy Sciences, Grant No. DE-FG02-09ER16089. We thank William Brennessel for assistance with X-ray crystallography.

■ REFERENCES

(1) Trnka, T. M.; Grubbs, R. H. *Acc. Chem. Res.* **2000**, *34*, 18.
(2) Martin, R.; Buchwald, S. L. *Acc. Chem. Res.* **2008**, *41*, 1461.
(3) Hahn, F. E.; Jahnke, M. C. *Angew. Chem., Int. Ed.* **2008**, *47*, 3122.
(4) Díez-González, S.; Marion, N.; Nolan, S. P. *Chem. Rev.* **2009**, *109*, 3612.
(5) Jones, W. D. *J. Am. Chem. Soc.* **2009**, *131*, 15075.
(6) Dröge, T.; Glorius, F. *Angew. Chem., Int. Ed.* **2010**, *49*, 6940.
(7) Dorta, R.; Stevens, E. D.; Scott, N. M.; Costabile, C.; Cavallo, L.; Hoff, C. D.; Nolan, S. P. *J. Am. Chem. Soc.* **2005**, *127*, 2485.
(8) Chianese, A. R.; Li, X.; Janzen, M. C.; Faller, J. W.; Crabtree, R. H. *Organometallics* **2003**, *22*, 1663.
(9) Tolman, C. A. *Chem. Rev.* **1977**, *77*, 313.
(10) Cavallo, L.; Correa, A.; Costabile, C.; Jacobsen, H. *J. Organomet. Chem.* **2005**, *690*, 5407.
(11) Clavier, H.; Nolan, S. P. *Chem. Commun.* **2010**, *46*, 841.
(12) Marion, N.; Navarro, O.; Mei, J.; Stevens, E. D.; Scott, N. M.; Nolan, S. P. *J. Am. Chem. Soc.* **2006**, *128*, 4101.
(13) Benkeser, R. A.; Schroeder, W. *J. Am. Chem. Soc.* **1958**, *80*, 3314.
(14) Clapp, D. B. *J. Am. Chem. Soc.* **1939**, *61*, 523.
(15) Huang, J.; Nolan, S. P. *J. Am. Chem. Soc.* **1999**, *121*, 9889.
(16) Böhm, V. P. W.; Weskamp, T.; Gstöttmayr, C. W. K.; Herrmann, W. A. *Angew. Chem., Int. Ed.* **2000**, *39*, 1602.
(17) Arduengo, A. J.; Krafczyk, R.; Schmutzler, R.; Craig, H. A.; Goerlich, J. R.; Marshall, W. J.; Unverzagt, M. *Tetrahedron* **1999**, *55*, 14523.

(18) Poater, A.; Cosenza, B.; Correa, A.; Giudice, S.; Ragone, F.; Scarano, V.; Cavallo, L. *Eur. J. Inorg. Chem.* **2009**, 1759.
(19) Guzei, I. A.; Wendt, M. *Dalton Trans.* **2006**, 3991.
(20) Guzei, I. A.; Wendt, M. *Solid-G*; University of Wisconsin: Madison, WI, 2004.
(21) Blue, E. D.; Gunnoe, T. B.; Petersen, J. L.; Boyle, P. D. *J. Organomet. Chem.* **2006**, *691*, 5988.
(22) Stasch, A.; Singh, S.; Roesky, H. W.; Noltemeyer, M.; Schmidt, H.-G. *Eur. J. Inorg. Chem.* **2004**, 4052.
(23) Miyaura, N.; Suzuki, A. *Chem. Rev.* **1995**, *95*, 2457.
(24) Barder, T. E.; Walker, S. D.; Martinelli, J. R.; Buchwald, S. L. *J. Am. Chem. Soc.* **2005**, *127*, 4685.
(25) Navarro, O.; Marion, N.; Mei, J.; Nolan, S. P. *Chem.—Eur. J.* **2006**, *12*, 5142.
(26) Altenhoff, G.; Goddard, R.; Lehmann, C. W.; Glorius, F. *Angew. Chem., Int. Ed.* **2003**, *42*, 3690.
(27) Ragone, F.; Poater, A.; Cavallo, L. *J. Am. Chem. Soc.* **2010**, *132*, 4249.
(28) Würtz, S.; Glorius, F. *Acc. Chem. Res.* **2008**, *41*, 1523.
(29) Lavallo, V.; Canac, Y.; Präsang, C.; Donnadieu, B.; Bertrand, G. *Angew. Chem., Int. Ed.* **2005**, *44*, 5705.
(30) Sakata, T.; Maruyama, S.; Ueda, A.; Otsuka, H.; Miyahara, Y. *Langmuir* **2007**, *23*, 2269.
(31) Zhang, W.; Yamamoto, H. *J. Am. Chem. Soc.* **2006**, *129*, 286.
(32) Tang, Y.; Zakharov, L. N.; Rheingold, A. L.; Kemp, R. A. *Inorg. Chim. Acta* **2006**, *359*, 775.
(33) Hong, S. Personal communication.
(34) Genov, M.; Almorín, A.; Espinet, P. *Chem.—Eur. J.* **2006**, *12*, 9346.